Asian Journal of Information Technology 15 (8): 1340-1348, 2016
ISSN: 1682-3915

Closed Loop Controlled Nine Level Inverter Fed Induction Motor Drive Using an Artificial Neural Network

[1]D. Jasmine and [2]M. Gopinath,
[1]Department of Electrical and Electronics Engineering, St. Peter's University, Chennai, India
[2]Department of Electrical and Electronics Engineering, Dr.N.G.P. Institute of Technology, Coimbatore, Tamil Nadu, India

Abstract: In airconditioner system, multilevel inverter fed single phase motor is preferred because of low THD. This research deals with the modelling and the simulation of closed loop controlled PV based boost-boost converter cum MLI system. The ANN controller is proposed to improve the dynamic response. The output voltage of PV system is boosted using a cascaded boost converter and it is inverted using a nine level inverter. The circuit configuration and Simulink modules are presented. The simulation results of open loop system, closed loop system with PI controller and ANN controller are presented. The responses of PI and ANN controlled systems are compared. The Neural network controller is proposed to improve the dynamic response of the system. The hardware is engineered and the obtained experimental results are compared with the simulation results.

Key words: Solar power, MLI, boost converter, PI controller, closed loop control, artificial neural network

INTRODUCTION

The extensive use of fossil fuels has resulted in the global problem of greenhouse emissions. Moreover, as the supplies of fossil fuels are depleted in the future they will become increasingly expensive. Thus, solar energy is becoming more important since it produces less pollution and the cost of fossil fuel energy is rising, while the cost of solar arrays is decreasing. In particular, small-capacity distributed power generation systems using solar energy may be widely used in residential applications in the near future (Mastromauro *et al*., 2012; Zhao *et al*., 2012).

The power conversion interface is important to grid- connected solar power generation systems because it converts the DC power generated by a solar cell array into AC power and feeds this AC power into the utility grid. An inverter is necessary in the power conversion interface to convert the DC power to AC power (Zhao *et al*., 2012; Hanif *et al*., 2011; Shen *et al*., 2012). Since, the output voltage of a solar cell array is low, a DC-DC power converter is used in a small-capacity solar power generation system to boost the output voltage, so it can match the DC bus voltage of the inverter. The power conversion efficiency of the power conversion interface is important to in- sure that there is no waste of the energy generated by the solar cell array. The active devices and passive devices in the inverter produce a power loss. The power losses due to active devices include both conduction losses and switching losses. Conduction loss results from the use of active devices, while the switching loss is proportional to the voltage and the current changes for each switching and switching frequency. A filter inductor is used to process the switching harmonics of an inverter, since the power loss is proportional to the amount of switching harmonics.

The voltage change in each switching operation for a multi- level inverter is reduced in order to improve its power conversion efficiency (Hasegawa and Akagi, 2012; Pouresmaeil *et al*., 2012; Srikanthan and Mishra, 2010; Chaves *et al*., 2010; Barros *et al*., 2013; Sadigh *et al*., 2010; Thielemans *et al*., 2012; Choi and Saeedifard, 2012; Maharjan *et al*., 2012; She *et al*., 2012) and the switching stress of the active devices. The amount of switching harmonics is also attenuated and the power loss caused by the filter inductor is also reduced. Therefore, multilevel inverter technology has been the subject of much research over the past few years. In theory, multilevel inverters should be designed with higher voltage levels in order to improve the conversion efficiency and to reduce harmonic content and Electro Magnetic Interference (EMI).

Conventional multilevel inverter topologies include the diode-clamped (Hasegawa and Akagi, 2012; Pouresmaeil *et al*., 2012; Srikanthan and Mishra, 2010; Chaves *et al*., 2010; Barros *et al*., 2013) the flying-capacitor (Sadigh *et al*., 2010; Thielemans *et al*.,

Corresponding Author: D.Jasmine, Department of Electrical and Electronics Engineering, St. Peter's University, Chennai, India

2012; Choi and Saeedifard, 2012) and the cascade H-bridge (Maharjan *et al*., 2012; She *et al*., 2012; Chavarria *et al*., 2013; Pereda and Dixon, 2011; Rahim *et al*., 2011) types. Diode-clamped and flying-capacitor multilevel inverters use capacitors to develop several voltage levels. But, it is difficult to regulate the voltage of these capacitors. Since, it is difficult to create an asymmetric voltage technology in both the diode-clamped and the flying-capacitor topologies, the power circuit is complicated by the increase in the voltage levels that is necessary for a multilevel inverter. For a single-phase seven-level inverter, 12 power electronic switches are required in both the diode-clamped and the flying-capacitor topologies. Asymmetric voltage technology is used in the cascade H-bridge multilevel inverter to allow more levels of output voltage (Pereda and Dixon, 2011). The cascade H-bridge multilevel inverter is suitable for applications with increased voltage levels. Two H-bridge inverters with a DC bus voltage of multiple relationships can be connected in cascade to produce a single- phase seven-level inverter and eight power electronic switches are used. More recently, various novel topologies for seven- level inverters have been proposed. For example, a single-phase seven-level grid-connected inverter has been developed for a photovoltaic system (Rahim *et al*., 2011). This seven-level grid-connected inverter contains six power electronic switches. However, three DC capacitors are used to construct the three voltage levels which results in that balancing the voltages of the capacitors is more complex. In a seven-level inverter topology, configured by a level generation part and a polarity generation part is proposed (Ounejjar *et al*., 2012).

Power electronic switches of the level generation part operate at high frequency but, ten power electronic switches and three DC capacitors are required. The modular multilevel inverter is similar to the cascade H-bridge type. For this, a new modulation method is proposed to achieve dynamic capacitor voltage balance. In (Abdalla *et al*., 2013), a multilevel DC-link inverter is presented to overcome the problem of partial shading of individual photovoltaic sources that are connected in series. The DC bus of a full-bridge inverter is configured by several individual DC blocks, where each DC block is composed of a solar cell, a power electronic switch and a diode. Controlling the power electronics of the DC blocks will result in a multilevel DC-link voltage to supply a full-bridge inverter and to simultaneously overcome the problems of partial shading of individual photovoltaic sources. To the best of authors knowledge, the literature does not deal with cascaded boost converter nine level inverter based PV system.

According to the knowledge of the authors, the comparison between PI and ANN controlled MLI fed IM systems is not reported in the papers. This study proposes a new ANN based solar power generation system. The proposed solar power generation system is composed of a DC/DC power converter and a nine-level inverter. The nine-level inverter is configured using a capacitor selection circuit and a full-bridge power converter, connected in cascade. The nine-level inverter contains only eight power electronic switches, which simplifies the circuit configuration.

MATERIALS AND METHODS

Circuit configuration: Figure 1 shows the configuration of the proposed solar power generation system. The proposed solar power generation system is composed of a solar cell array, a DC-DC power converter and a nine-level inverter. The solar cell array is connected to the DC-DC power converter and the DC-DC power converter is a boost converter that incorporates a transformer. The DC–DC power converter converts the

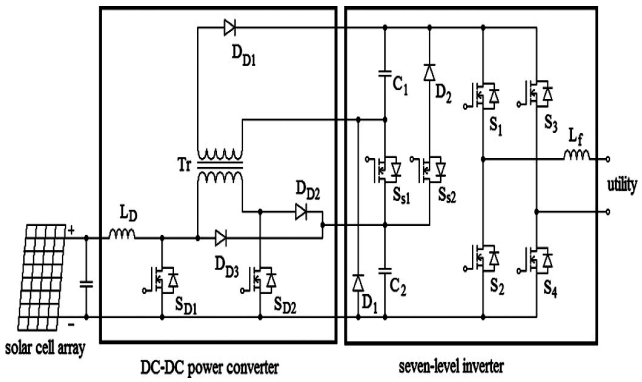

Fig. 1: Configuration of the solar power generation system

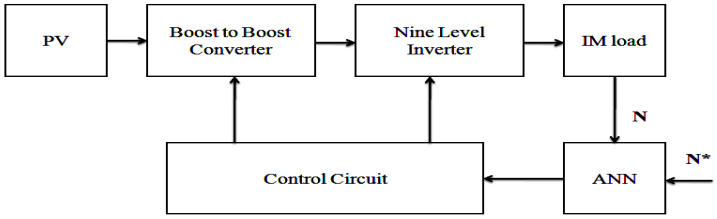

Fig. 2: Block diagram of the proposed system

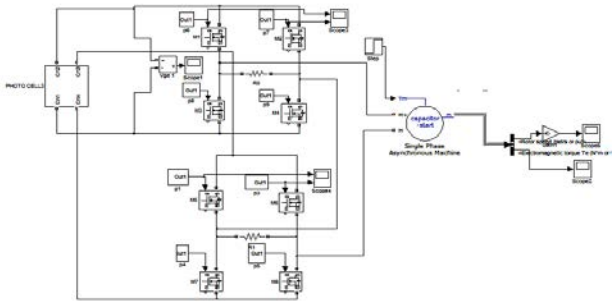

Fig. 3: Simulink model of the open loop system with step change in load torque

Table 1: Simulation paramerters

Perameters	Values
Vin	48V
L1	100mH
C1	2500µF
RL	5KΩ
MOSFET IRF840	500V 8A^{-1}
DIODE	230V 1A^{-1}
Vo	100V

output power of the solar cell array into two independent voltage sources with Multiple relationships which are supplied to the seven level inverter. This new nine-level inverter is Composed of a capacitor selection circuit and a full bridge power converter, connected in a cascade. The power electronic switches of capacitor selection circuit determine the discharge of the two capacitors while the two capacitors are being discharged individually or in series. Because of the multiple relationships between the voltages of the DC capacitors, the capacitor selection circuit outputs a three-level DC voltage. Actual speed is compared with the set speed and the error is applied to the controller. The pulse width of boost to boost converter is updated to maintain constant speed (Fig. 2):

$$v_o = \sum_{j=1}^{n} v_j s_j$$

Where: S = Is switching function of jth node:

T= Tfo-Tba

Simulation: Nine level inverter fed single phase induction motor drive system is modelled and simulated in open loop and closed loop. The results of simulation in open loop and closed loop with ANN controller are discussed in Table 1.

The open loop controlled induction motor drive system with step change in load is shown in Fig. 3.The load torque is increased at t = 10 sec and hence the speed decreases to 1300RPM as shown in Fig. 4.

The Simulink model of closed loop control nine level inverter system with PI controller is shown in Fig. 5.The output voltage of the converter is shown in Fig. 6 and its value is 160V. The output voltage of the inverter is shown in Fig. 7. The peak value increases from 100V-200V. The speed response is shown in Fig. 8 and it can be seen that the speed reaches set value due to closed loop operation.

The Simulink model of closed loop system with neural network controller is shown in Fig. 9. The PI controller in closed loop is replaced by ANN controller. The inputs to the ANN controller are error and change in error. The output voltage of the converter is shown in Fig. 10. The output voltage of the inverter and speed response are shown in Fig. 11and 12 respectively. The speed reaches set value without any deviations. The

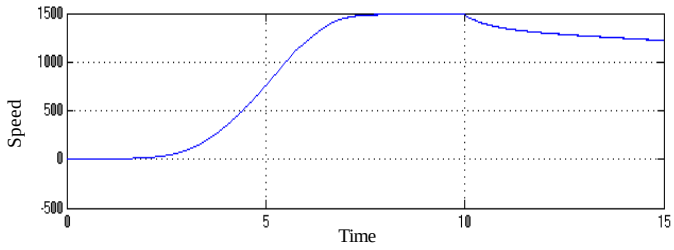

Fig. 4: Speed waveform

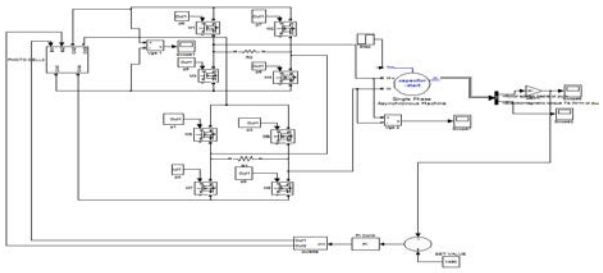

Fig. 5: Simulink model of the closed loop system with the PI controller

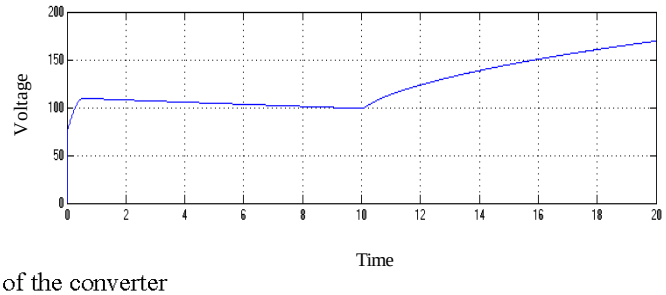

Fig. 6: Output voltage of the converter

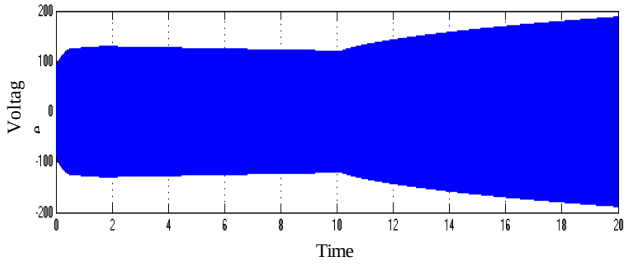

Fig. 7: Output voltage of the inverter

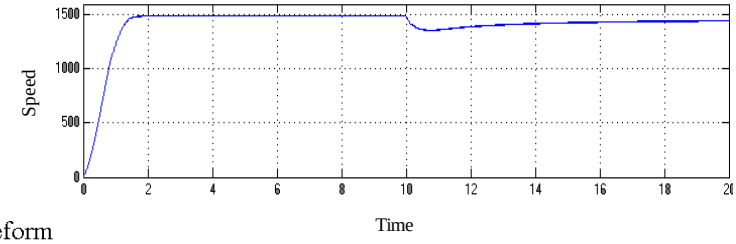

Fig. 8: Speed waveform

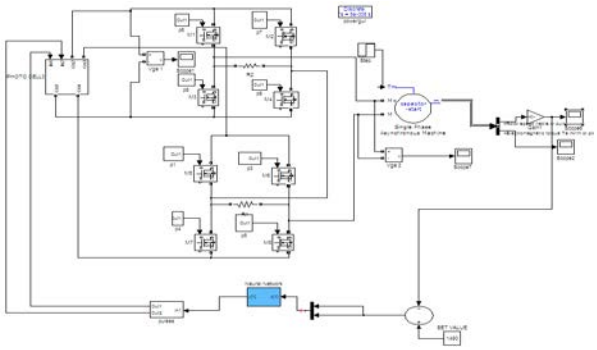

Fig. 9: Simulink model of the closed loop system with ANN controller

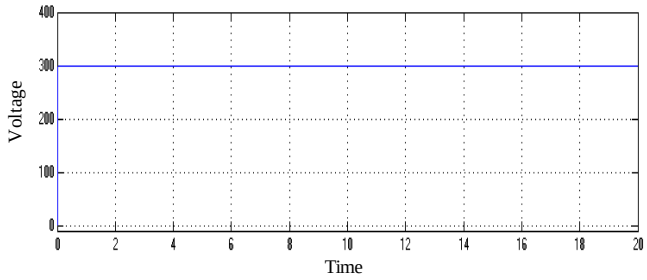

Fig. 10: Output voltage of the converter

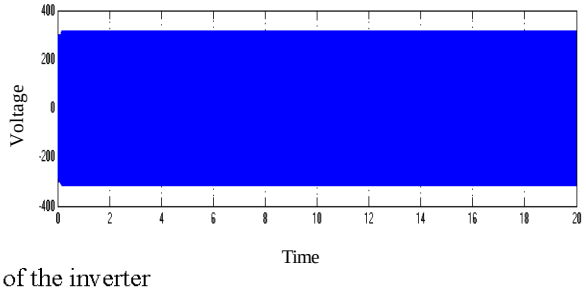

Fig. 11: Output voltage of the inverter

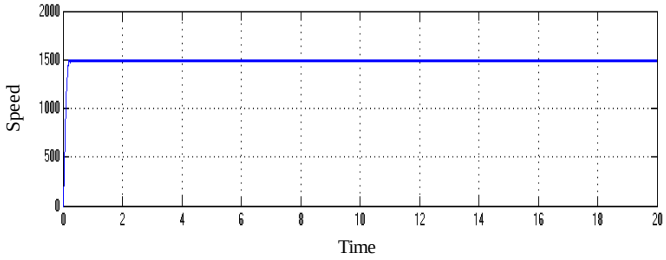

Fig. 12: Speed waveform

Table 2: Comparison of time domain parameters

Controllers	Rise time (s)	Peak times (s)	Settling time (s)	Steady state error (v)
PI controller	1.8	19	1.12	15
ANN	0.11	NA	NA	NA

comparison of time domain parameters with PI controller and ANN controller are shown in Table 2.

RESULTS AND DISCUSSION

The hardware for nine level based boost converter inverter system is engineered and tested in the lab.

The hardware setup consists of PV panel, control board, H-bridge 1, H-bridge 2 and load modules. The snapshot of the total hardware is shown in Fig. 13. The

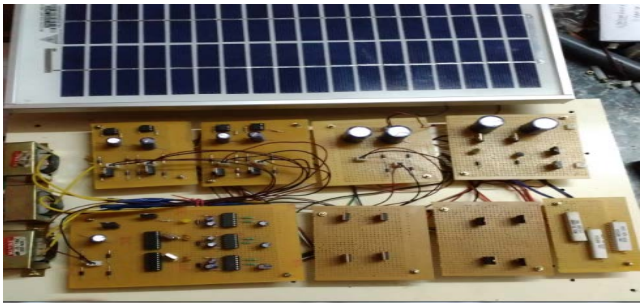

Fig. 13: Snapshot of total hradware

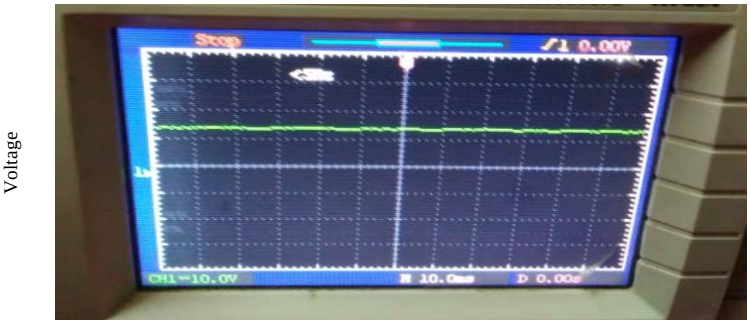

Fig. 14: Output voltage of the solar system; X-Asix 1 unit = 1ms; Y-Axis 1 unit = 5v

Fig. 15: Output voltage of the boots converter 1; X-Asix 1 unit = 1ms; Y-Axis 1 unit = 20v

Fig. 16: Output voltage of the boots converter 1; X-Asix 1 unit = 1ms; Y-Axis 1 unit = 20v

output voltage of solar system is shown in Fig. 14. The output voltage of boost converter 1 and boost converter 2 are shown in Figs. 15 and 16 respectively. The switching pulse from the PIC and output of driver for the switch M1 are shown in Fig. 17 and 18 respectively. The switching pulse and driver output for the device M3 are shown in Fig. 19 and 20, respectively. The output voltage of the multi level inverter is shown in the Fig. 21.

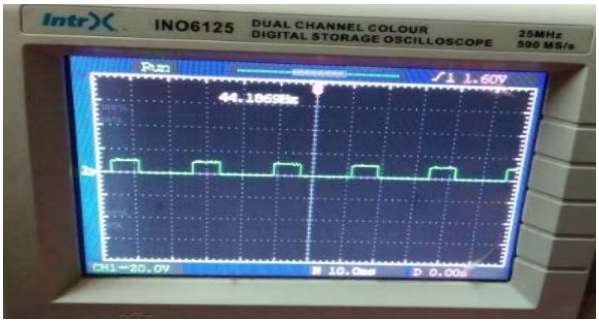

Fig. 17: Switching pulse from the PIC; X-Asix 1 unit = 1ms; Y-Axis 1 unit = 5v

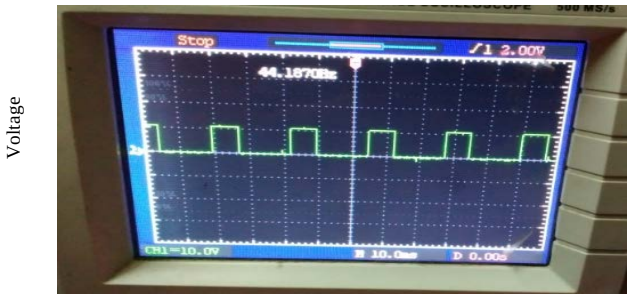

Fig. 18: Driver output for the switch M1; X-Asix 1 unit = 1ms; Y-Axis 1 unit = 10v

Fig. 19: Switching pulses for the device M3; X-Asix 1 unit = 1ms; Y-Axis 1 unit = 5v

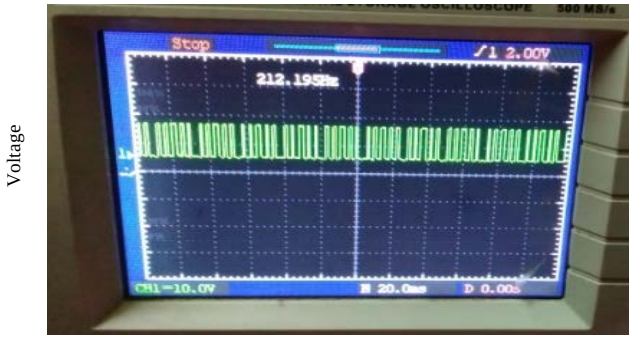

Fig. 20: Driver output for the device M3; X-Asix 1 unit = 1ms; Y-Axis 1 unit = 10v

Fig. 21: Output voltage of the multi level inverter; X-Asix 1 unit = 1ms; Y-Axis 1 unit = 20 v

CONCLUSION

The Boost-Boost converter fed nine level inverter system was modelled and simulated successfully controllers like PI and neural network were used to regulate the speed under variable insulation levels. The simulation results indicate that the response is smoother with ANN controller. The advantages of this system are reduction in the settling time and steady state error. The disadvantage of the system is that it require two boost converters and two H-bridges.

The experimental results validate the simulation results. The contribution of this work is to improve the dynamic response of drive system using ANN controller. This research deals with simulation of open loop and closed loop controlled systems using ANN. Closed loop system with FLC will be investigated in future. This system can also be controlled using FPGA to enhance the switching frequency.

NOMENCLATURE

MLI-Multi Level Inverter
PWM-Pulse Width Modulation
PI-Propotional Integral
THD-Total Harmonic Distortion
EMI-Electro Magnetic Interference
MOSFET-Metal Oxide Semi-conductor Field Effect Transistor
ANN-Artificial Neural Network

REFERENCES

Abdalla, I., J. Corda and L. Zhang, 2013. Multilevel DC-link inverter and control algorithm to overcome the PV partial shading. Power Electron. IEEE. Trans., 28: 14-18.

Barros, J.D., J.F.A. Silva and E.G. Jesus, 2013. Fast-predictive optimal control of NPC multilevel converters. Ind. Elect. IEEE. Trans., 60: 619-627.

Chavarria, J., D. Biel, F. Guinjoan, C. Meza J.J. Negroni, 2013. Energy-balance control of PV cascaded multilevel grid-connected inverters under level-shifted and phase-shifted PWMs. Ind. Electron. IEEE. Trans., 60: 98-111.

Chaves, M., E. Margato, J.F. Silva and S.F. Pinto, 2010. New approach in back-to-back m-level diodeclamped multilevel converter modelling and direct current bus voltages balancing. Power Electron. IET., 3: 578-589.

Choi, S. and M. Saeedifard, 2012. Capacitor voltage balancing of flying capacitor multilevel converters by space vector PWM. Power Delivery, IEEE. Trans., 27: 1154-1161.

Hanif, M., M. Basu and K. Gaughan, 2011. Understanding the operation of a Z-source inverter for photovoltaic application with a design example. Power Electron. IET., 4: 278-287.

Hasegawa, K. and H. Akagi, 2012. Low-modulation-index operation of a five-level diode-clamped PWM inverter with a dc-voltage-balancing circuit for a motor drive. Power Electron. IEEE. Trans., 27: 3495-3504.

Maharjan, L., T. Yamagishi and H. Akagi, 2012. Active-power control of individual converter cells for a battery energy storage system based on a multilevel cascade PWM converter. Power Electron. IEEE. Trans., 27: 1099-1107.

Mastromauro, R.A., M. Iserre and A. Quila, 2012. Control issues in single-stage photovoltaic systems: MPPT, current and voltage control. Ind. Inf. EEE. Trans., 8: 241-254.

Ounejjar, Y., K. Al-Haddad and L.A. Dessaint, 2012. A novel six-band hysteresis control for the packed U cells seven-level converter: Experimental validation. Ind. Electron. IEEE. Trans., 59: 3808-3816.

Pereda, J. and J. Dixon, 2011. High-frequency link: A solution for using only one DC source in asymmetric cascaded multilevel inverters. Ind. Electron. IEEE. Trans., 58: 3884-3892.

Pouresmaeil, E., D. Montesinos-Miracle and O. Gomis-Bellmunt, 2012. Control scheme of three-level NPC inverter for integration of renewable energy resources into AC grid. Syst. J. IEEE., 6: 242-253.

Rahim, N.A., K. Chaniago and J. Selvaraj, 2011. Single-phase seven-level grid-connected inverter for photovoltaic system. Ind. Electron. IEEE. Trans., 58: 2435-2443.

Sadigh, A.K., S.H. Hosseini, M. Sabahi and G.B. Gharehpetian, 2010. Double flying capacitor multicell converter based on modified phase-shifted pulsewidth modulation. Power Electron. IEEE. Trans., 25: 1517-1526.

She, X., A.Q. Huang, T. Zhao and G. Wang, 2012. Coupling effect reduction of a voltage-balancing controller in single-phase cascaded multilevel converters. Power Electron. IEEE. Trans., 27: 3530-3543.

Shen, J.M., H.L. Jou and J.C. Wu, 2012. Novel transformerless grid-connected power converter with negative grounding for photovoltaic generation system. Power Electron. IEEE. Trans., 27: 1818-1829.

Srikanthan, S. and M.K. Mishra, 2010. DC capacitor voltage equalization in neutral clamped inverters for DSTATCOM application. Ind. Electron. IEEE. Trans., 57: 2768-2775.

Thielemans, S., A. Ruderman, B. Reznikov and J. Melkebeek, 2012. Improved natural balancing with modified phase-shifted PWM for single-leg five-level flying-capacitor converters. Power Electron. IEEE. Trans., 27: 1658-1667.

Zhao, Z., M. Xu, Q. Chen, J.S. Lai and Y. Cho, 2012. Derivation, analysis and implementation of a boost-buck converter-based high-efficiency PV inverter. Power Electron. IEEE. Trans., 27: 1304-1313.